Behavioral/Cognitive

Maturational Indices of the Cognitive Control Network Are Associated with Inhibitory Control in Early Childhood

Philipp Berger,[1,2] Angela D. Friederici,[1] and Charlotte Grosse Wiesmann[2]
[1]Department of Neuropsychology, Max Planck Institute for Human Cognitive and Brain Sciences, Leipzig, 04103, Germany, and [2]Research Group Milestones of Early Cognitive Development, Max Planck Institute for Human Cognitive and Brain Sciences, Leipzig, 04103, Germany

Goal-directed behavior crucially relies on our capacity to suppress impulses and predominant behavioral responses. This ability, called inhibitory control, emerges in early childhood with marked improvements between 3 and 4 years. Here, we ask which brain structures are related to the emergence of this critical ability. Using a multimodal approach, we relate the pronounced behavioral improvements in different facets of 3- and 4-year-olds' ($N = 37$, 20 female) inhibitory control to structural indices of maturation in the developing brain assessed with MRI. Our results show that cortical and subcortical structure of core regions in the adult cognitive control network, including the PFC, thalamus, and the inferior parietal cortices, is associated with early inhibitory functioning in preschool children. Probabilistic tractography revealed an association of frontoparietal (i.e., the superior longitudinal fascicle) and thalamocortical connections with early inhibitory control. Notably, these associations to brain structure were distinct for different facets of early inhibitory control, often referred to as motivational ("hot") and cognitive ("cold") inhibitory control. Our findings thus reveal the structural brain networks and connectivity related to the emergence of this core faculty of human cognition.

Key words: **brain structure; cognitive control; executive function; inhibitory control**

Significance Statement

The capacity to suppress impulses and behavioral responses is crucial for goal-directed behavior. This ability, called inhibitory control, develops between the ages of 3 and 4 years. The factors behind this developmental milestone have been debated intensely for decades; however, the brain structure that underlies the emergence of inhibitory control in early childhood is largely unknown. Here, we relate the pronounced behavioral improvements in inhibitory control between 3 and 4 years with structural brain markers of gray matter and white matter maturation. Using a multimodal approach that combines analyses of cortical surface structure, subcortical structures, and white matter connectivity, our results reveal the structural brain networks and connectivity related to this core faculty of human cognition.

Introduction

The capacity to suppress impulses and behavioral responses is crucial for goal-directed behavior (Rothbart and Posner, 1985). This ability, called inhibitory control (IC), develops rapidly between the ages of 3 and 4 years (Petersen et al., 2016). The factors behind this developmental milestone have been debated for decades; however, the neurobiological correlates of the early development in IC are largely unknown. What are the brain structures related to this core faculty in human cognitive development?

In early childhood, the cerebral cortex undergoes complex developmental changes as a result of the interaction of microbiologic processes (Raznahan et al., 2011; Walhovd et al., 2017). These maturational processes, observed in changes of cortical and subcortical gray matter (GM) and in the interconnectedness through white matter (WM) pathways, have each shown robust associations with cognitive development in childhood (Johansen-Berg, 2010; Walhovd et al., 2017). The interrelation of GM and WM structure with cognitive function, however, has only rarely been studied in the first years of life, given the difficulty to conduct high-resolution MRI in this age group (but see Cafiero et al., 2019). Therefore, to date, only little is known about the neural maturation processes underlying the emergence of IC in early childhood, particularly in the early preschool period from 3 years of age that marks a critical take-off in IC abilities.

Received Nov. 8, 2021; revised May 20, 2022; accepted May 24, 2022.

Author contributions: P.B. and C.G.W. analyzed data; P.B. wrote the first draft of the paper; P.B., A.D.F., and C.G.W. edited the paper; A.D.F. and C.G.W. designed research; C.G.W. performed research.

We thank Julia Werner, Anne Grigutsch, Lisa Uhlich, and Alina Kowald for help with correcting segmentation and surface reconstruction in FreeSurfer; and Hung Nguyen Trong and Christiane Attig for help with data acquisition and organization.

The authors declare no competing financial interests.

Correspondence should be addressed to Philipp Berger at berger@cbs.mpg.de.

https://doi.org/10.1523/JNEUROSCI.2235-21.2022

In adults and older children, fMRI studies have revealed that mature cognitive control is supported by a neural network of prefrontal and parietal cortices, along with subcortical structures (including the ventral striatum and thalamus), referred to as the superordinate cognitive control network (sCCN) (Niendam et al., 2012; McKenna et al., 2017). In addition, connections between subcortical and the relevant cortical regions were shown to be involved in mature IC (Somerville and Casey, 2010; Halassa and Kastner, 2017). Studies in middle childhood and adolescence suggest some continuity of the functional involvement of the sCNN and PFC in cognitive control, at least from late childhood into adolescence (see McKenna et al., 2017; Fiske and Holmboe, 2019). For younger children, there is evidence from functional near-infrared spectroscopy studies for a similar frontoparietal network to be functionally involved between the age of 3 and 6 years (Mehnert et al., 2013; Buss and Spencer, 2018; Moriguchi et al., 2018; Moriguchi, 2022). These findings suggest that the brain-structural maturation of the sCCN may be associated with the emergence of early IC.

In behavioral studies on early IC development, different facets of inhibition have been described (Simpson and Carroll, 2019), including a distinction between inhibition in neutral and emotional task contexts, referred to as "cold" and "hot" IC (Zelazo and Carlson, 2012; Montroy et al., 2019). Neuroimaging research in adults and older children has largely focused on inhibition under motivationally neutral ("cold") task conditions. A standard "cold" inhibition measure is the Go-NoGo task. In this task, children are required to perform a simple motor response when a stimulus is shown and to withhold this response when seeing another stimulus. Another line of the developmental research, in contrast, has focused on inhibition in emotional high-stake ("hot") situations. The standard task for this domain of IC is the Delay of Gratification tasks (Mischel et al., 1989). In this task, children are required to resist their impulse to choose an immediate reward in favor of a delayed larger reward. Although the distinction between "hot" and "cold" IC is widely recognized in the behavioral developmental literature, it is debated whether, despite the conceptual differences in task designs, these components share a common basis or address distinct and independent cognitive processes (Simpson and Carroll, 2019). From a neural perspective, studies in adults suggest that performance in the Delay of Gratification task might relate to a different functional network, including the orbitofrontal cortex (OFC) and frontostriatal connections (Casey et al., 2011). Studies in children, in turn, have reported functional recruitment of the lateral PFC (Moriguchi et al., 2018).

In the present study, we use high-resolution MRI to investigate how structural markers of brain maturation in GM and WM are related to early IC in the preschool period. In particular, we relate behavioral indices of different facets of early IC to structural properties of the PFC, OFC, and more broadly the sCCN, investigating cortical and subcortical structures in combination with WM connectivity in the critical age of 3-4 years when IC emerges.

Materials and Methods

Participants

MRI data and behavioral data of 37 typically developing 3- and 4-year-old children were analyzed for the present study (17 children age 3.07-3.59 years, median = 3.33, SD = 0.18, 10 female; and 20 children age 4.02-4.58 years, median = 4.29, SD = 0.18, 10 female). The sample size was estimated based on previous developmental MRI studies with ~20 children per age group, assuming a dropout rate of 10%-20% because of motion artifacts. Thus, the behavioral assessment was conducted in a total sample of $n = 60$ children age 3 and 4 years (Grosse Wiesmann et al., 2017a) from which we excluded children because they (1) did not participate in both IC tasks ($n = 1$), (2) did not participate in or aborted the MRI ($n = 9$), (3) showed incidental neurologic findings ($n = 1$), (4) showed motion artifacts in the sMRI data ($n = 11$) (Grosse Wiesmann et al., 2020), or (5) dMRI data (Grosse Wiesmann et al., 2017b; for details, see the respective sections on sMRI/dMRI data analysis). One additional child was excluded because of an MRI acquisition error. Parental informed consent was obtained for all children, and the study was approved by the Ethics Committee at the Faculty of Medicine of the University of Leipzig.

Assessment of IC

The children performed two standard tests of "cold" and "hot" IC: a Go-NoGo task (Rakoczy, 2010) and a Delay of Gratification task (Mischel and Ebbesen, 1970), which have been described in detail in previous studies (Grosse Wiesmann et al., 2017a,b). Briefly, in the Go-NoGo task, children were asked to perform actions a duck puppet asked them to do (for example, 'Clap your hands!'), but not to do anything the nasty crocodile asked them to. A d' value was calculated with correct NoGo-trials as hits and incorrect Go-trials as false alarms (mean = 0.875, SD = 0.178). One child had to be excluded from further analyses because the child did not provide complete data on the task. For the Delay of Gratification task, children asked to wait in front of highly desirable object (gummy bears or chocolate bars) for 5 min to receive a bigger reward. One child had to be excluded from further analyses because the child did not provide complete data on the task. The children's mean waiting time was mean = 226 s (SD = 111 s). To ensure comparability across task scores, we computed standardized scores of task performance in the Go-NoGo task and the Delay of Gratification task. The data on these tasks were non-normally distributed because of the developmental breakthrough observed in the age range between 3 and 4 years. Therefore, we made sure that the statistical tests conducted were either nonparametric or that the data met the assumptions (i.e., normality of residuals).

MRI data acquisition

MRI data were acquired on a 3-T Siemens scanner (Siemens MRT Trio series) using a 32-channel head coil. The acquisition protocols are described in detail in previous studies (Grosse Wiesmann et al., 2017b, 2020). High-resolution 3D T1-weighted MRI images were acquired using the MP2RAGE sequence (Marques et al., 2010) at $1.2 \times 1 \times 1$ mm resolution (Grosse Wiesmann et al., 2020). Furthermore, dMRI data were acquired using the multiplexed EPI sequence (Feinberg et al., 2010) with a resolution of 1.9 mm isotropic (Grosse Wiesmann et al., 2017b). A field map was acquired directly after the dMRI scan.

sMRI data analysis

Cortical surface-based analyses. To obtain measures of cortical thickness and surface area, we used the preprocessed brain images from a recent study using the current dataset (Grosse Wiesmann et al., 2020). In short, individual brain images were preprocessed in FreeSurfer 5.3.0 (http://surfer.nmr.mgh.harvard.edu) to reconstruct cortical surfaces and generate local estimates of cortical thickness and surface area following the standard surface-based stream (Fischl and Dale, 2000). Using a standardized workflow to detect motion artifacts (Backhausen et al., 2016), $n = 11$ children were excluded after initial screening, only including data of participants that had good to moderate MRI scans. Further, as recommended in the FreeSurfer pipeline (http://surfer.nmr.mgh.harvard.edu/fswiki/FsTutorial/TroubleshootingData), the outputs of skull stripping, WM segmentation, and cortical and pial surfaces were inspected visually for errors and corrected manually when necessary. The automated FreeSurfer pipeline was rerun for the surfaces that contained errors and then reinspected (Backhausen et al., 2016). Surface area of the GM/WM boundary and cortical thickness, defined as the closest distance from the GM/WM boundary to the GM/CSF

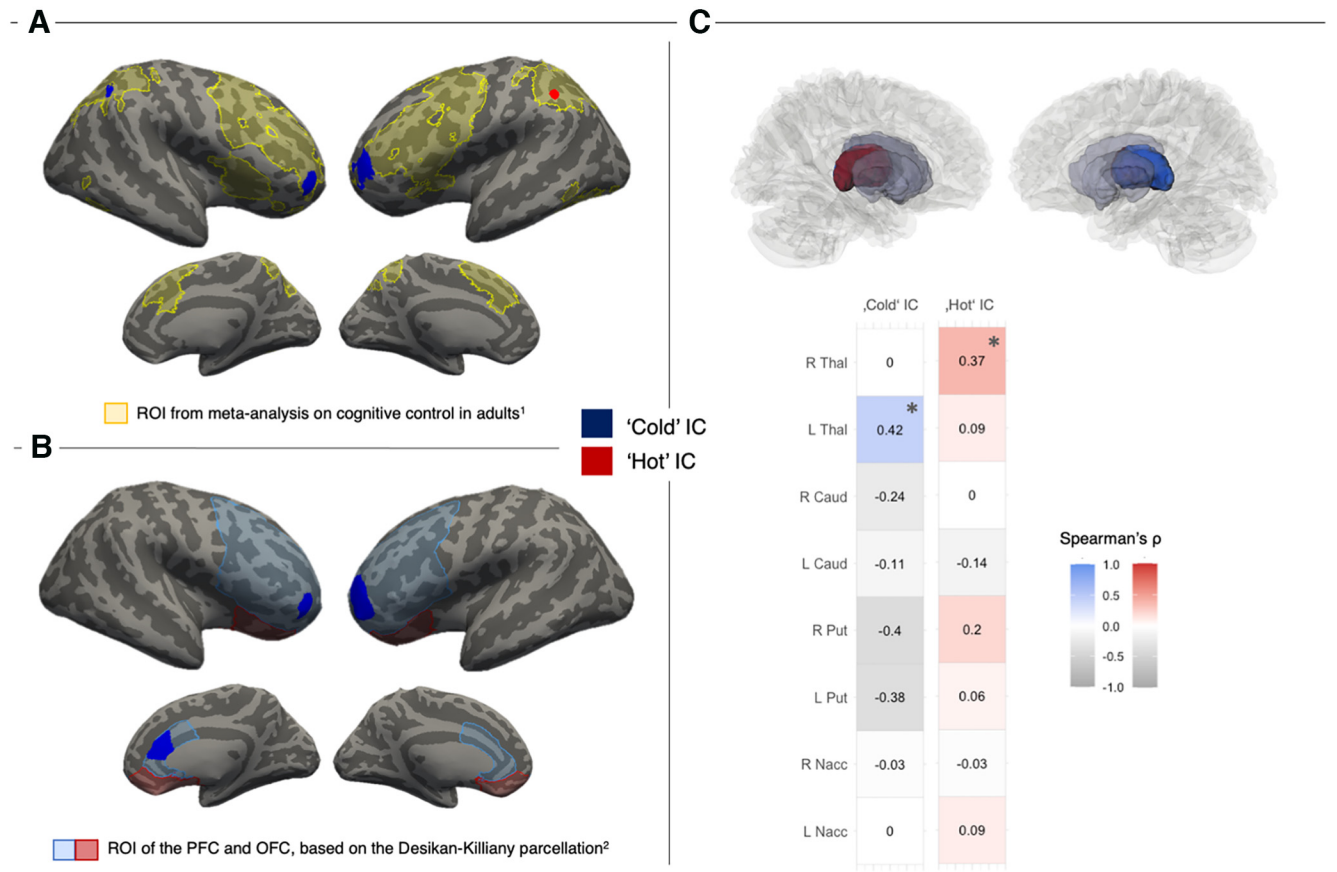

Figure 1. Relation of "cold" (blue) and "hot" (red) IC performance with cortical surface area and subcortical volume. ***A***, Small-volume corrected linear relation of "cold" IC performance (blue) with surface area in bilateral RFC (BA10) and right inferior parietal lobe and "hot" IC performance (red) with cortical surface area in the left supramarginal gyrus within the regions of the sCCN (light yellow). ***B***, Small-volume corrected linear relation of "cold" IC performance with surface area in the caudal ACC within the PFC mask (light blue) and medial OFC within the OFC mask (light red). All effects on the cortical surface are independent of children's age and gender, and cluster-size corrected at $p < 0.05$. ***C***, Results of nonparametric partial correlation analyses of "cold" and "hot" IC performance with volume of subcortical structures, color-coded for strength of positive association. A significant positive correlation of "cold" IC (blue) with volume of the left thalamus, and "hot" IC (red) with the right thalamus was revealed. These relations were independent of children's chronological age and gender. Thal, Thalamus; Caud, caudate nucleus; Put, putamen; Nacc, nucleus accumbens.

boundary, was calculated at each vertex. The resulting maps for cortical thickness and surface area were smoothed on the tessellated surfaces using a 10 mm FWHM Gaussian kernel. A common group template was created from the individual T1-weighted images of all children included in the analysis using ANTs (Avants et al., 2008). The individual cortical surfaces were registered to the common group template to allow for an accurate matching of local cortical thickness and surface area measures across participants.

Subcortical volume analysis. Individual brain images were processed in FreeSurfer 7.0.0 (http://surfer.nmr.mgh.harvard.edu) to reconstruct subcortical volumes following the standard volume-based processing stream in FreeSurfer. The volume-based FreeSurfer processing stream conducts segmentation of several subcortical structures, including the thalamus and striatum. Based on our hypotheses, we restricted subsequent analyses to the bilateral thalamus and structures of the striatum, including the bilateral putamen, bilateral caudate nucleus, and bilateral nucleus accumbens. Quality control assessments of the thalamic and striatal reconstructions were conducted by two independent raters, yielding an interrater reliability of $M_{ICC} = 0.70$ (SD = 0.08). If the two raters agreed on a structure to show failures in segmentation, this structure was excluded from the statistical analyses for the individual participant. This procedure resulted in the exclusion of the following number of participants per structure: $N = 1$ for the left caudate nucleus, $N = 2$ for the right caudate nucleus, $N = 2$ for the left putamen, $N = 2$ for the right putamen, $N = 5$ for the left nucleus accumbens, $N = 6$ for right nucleus accumbens, $N = 1$ for the left thalamus, and $N = 1$ for right thalamus.

Statistical analysis. The relation of cortical thickness and surface area, respectively, with our main variables ("cold" and "hot" IC) were estimated in GLMs using the tool mri_glmfit implemented in FreeSurfer. In the GLMs, we controlled for children's chronological age and gender. Multiple comparison correction was applied with a clusterwise correction using the FreeSurfer tool mri_glmfit-sim, specifying a cluster-forming threshold of $p < 0.005$, clusterwise threshold of $p < 0.05$ (Greve and Fischl, 2018), positive relation with surface area, bidirectional relation with cortical thickness, and additional correction for the analyses on two hemispheres (Grosse Wiesmann et al., 2020). For the clusterwise correction, a Monte Carlo simulation with 10,000 iterations was precomputed on the group template. Given our hypotheses for neural networks associated with "cold" and "hot" IC, respectively, we computed additional analyses using small-volume correction. In particular, we used a binarized map of the sCCN, derived from a meta-analysis on "cold" inhibitory functioning in adults (Niendam et al., 2012). For this, we registered the original meta-analysis maps from the MNI space to our group template with the ANTs script WarpImageMultiTransform (http://stnava.github.io/ANTs/) and then projected them on the surface using the FreeSurfer tool mri_vol2surf (see Fig. 1*A*). Furthermore, based on our specific hypotheses for PFC and OFC, we selected these as ROIs based on the Desikan-Killiany parcellation (Desikan et al., 2006). The linear models for the relations of cortical thickness and surface area with "cold" and "hot" IC, respectively (as well as the analyses that included the covariates described above), were computed within the obtained masks with mri_glmfit as before. We checked for the normality of residuals using Kolmogorov–Smirnov tests.

The relation of subcortical volume of the thalamus and striatum with IC scores was assessed with nonparametric partial correlation analysis, using the 'ppcor' package (Kim, 2015) in R (R Core Team, 2019). In the analysis, we used a one-sided (positive) test to indicate significant correlations, while controlling for children's chronological age, gender, and estimated total intracranial volume, additionally correcting for the number of structures via false discovery rate (Benjamini and Hochberg, 1995).

dMRI data analysis

dMRI data processing. To obtain measures of WM connectivity, we used the preprocessed dMRI data and analysis pipeline from another study using the current dataset (Grosse Wiesmann et al., 2017b). To ensure reliable data quality, children were excluded if >10 of 60 acquired directions in the dMRI dataset were corrupted. Directions were removed because of intensity dropout caused by head motion (Schreiber et al., 2014) or because of artifacts detected in a visual inspection (Tournier et al., 2011; Soares et al., 2013). After removing motion artifacts manually, motion itself was corrected for by rigidly aligning all volumes to the last one without diffusion weighting (b0) using flirt from the FSL software package (Jenkinson et al., 2002). Subsequently, the motion-corrected dMRI data were rigidly aligned to the anatomic image, which again had been rigidly aligned to the MNI standard space and was interpolated to 1 mm isotropic voxel space. Distortions were corrected using the corresponding field map.

Seed region derivation. To see within which tracts the significant clusters from the sMRI analyses were located, these regions were taken as seeds for probabilistic tractography. For this, we projected the significant regions derived in the cortical surface-based and volume-based analysis on the GM/WM boundary in the individual subject's brain using the FreeSurfer tool label2label. After transforming the label files to volume, we rigidly aligned them to the diffusion space using flirt from the FSL software package (Jenkinson et al., 2002). In addition, a supplementary analysis was performed focusing only on frontostriatal connectivity. As a seed region for probabilistic tractography, we used a mask of the OFC, based on the Desikan-Killiany parcellation in FreeSurfer. Further, we defined an inclusion ROI combining FreeSurfer segmentations of bilateral caudate nucleus, putamen, and nucleus accumbens, yielding that only tracks that enter the inclusion ROI will be produced.

Statistical analysis. Tractography was run with MRtrix (Tournier et al., 2012) using Constrained Spherical Deconvolution as a local model (Tournier et al., 2004) with the default parameters, as in Grosse Wiesmann et al. (2017b). This procedure resulted in streamline density maps for each seed region and subject, in addition producing a map including only frontostriatal connections. To ensure that the identified correlations were not outlier-driven, we masked the streamline density maps of the individual subjects with a common group mask imposing that at least half the subjects have nonzero values in every voxel. The individual subjects' masked streamline density maps were then correlated with IC scores using GLMs with nonparametric permutation tests in FSL randomize (Winkler et al., 2014), while controlling for the mean volume in the seed region of the tractography. This was done to ensure that correlations with streamline density were not driven by the correlation of the IC score and GM structure found in the sMRI analysis. In addition, we controlled for age and gender by including them as covariates in the linear model. Reported clusters in the tract volumes were significant at $p < 0.005$ at voxel level and exceeded a cluster size significant at $p < 0.05$, in addition taking into account the number of streamline density maps according to Bonferroni correction. We localized and named the clusters and tracts based on the MRI Atlas of Human White Matter (Oishi et al., 2011).

Results

Behavioral results

A behavioral assessment of "hot" and "cold" inhibitory functioning and codeveloping cognitive functions was conducted in 60 children 3-4 years of age (Grosse Wiesmann et al., 2017a), from which a subsample of 37 children with usable MRI data were analyzed with respect to cortical brain structure (for details, see Materials and Methods). The children performed two standard tasks for "cold" and "hot" inhibitory functioning: a Go-NoGo task and a Delay of Gratification task (for details, see Materials and Methods). Performance in the "cold" IC task showed a significant correlation with age (Spearman's $\rho = 0.45$, $p < 0.001$), with 4-year-olds (mean = 0.94, SD = 0.10) performing significantly better than 3-year-olds (mean = 0.74, SD = 0.31; Mann–Whitney U test, $U = 202.50$, $p < 0.001$, $\eta^2 = 0.20$). Similarly, performance in the "hot" IC task showed a significant correlation with age (Spearman's $\rho = 0.38$, $p = 0.003$), with 4-year-olds (mean = 246.13 s, SD = 94.62) performing significantly better than 3-year-olds (mean = 183.96 s, SD =119.35; Mann–Whitney U test, $U = 296.50$, $p = 0.039$, $\eta^2 = 0.07$). No significant correlation between "hot" and "cold" IC performance was found (Spearman's $\rho = 0.17$, $p = 0.224$).

Analysis of cortical brain structure

To test whether IC performance was related to cortical brain structure, we reconstructed cortical surface area and thickness from high-resolution anatomic MRI in the same children that participated in the behavioral task battery.

"Cold" IC and cortical brain structure (Go-NoGo task)

On the whole brain, we observed a positive correlation of children's "cold" IC performance with their cortical surface area in the left rostral frontal cortex (RFC, BA 10; $r = 0.43$, clusterwise $p = 0.005$), inferior temporal gyrus ($r = 0.54$, clusterwise $p = 0.010$), precentral gyrus ($r = 0.45$, clusterwise $p = 0.022$), and right posterior cingulate cortex (Table 1; $r = 0.48$, clusterwise $p = 0.009$). Given our *a priori* hypotheses based on the brain regions relevant for "cold" IC in adults, we additionally computed small-volume corrections within the regions of the sCCN (as reported by Niendam et al., 2012) and the PFC. In addition to an effect in the left RFC ($r = 0.34$, clusterwise $p < 0.001$), this showed a positive correlation of children's "cold" IC performance with their cortical surface area in the right RFC ($r = 0.36$, clusterwise $p = 0.001$), right inferior parietal lobe (IPL; $r = 0.39$, clusterwise $p = 0.015$), and in the caudal ACC ($r = 0.46$, clusterwise $p = 0.001$; Table 1; Fig. 1*A*,*B*). All effects remained significant when controlling for chronological age and gender. There were no significant effects for cortical thickness.

"Hot" IC and cortical brain structure (Delay of Gratification task)

To identify cortical brain structure associated with "hot" IC development, we computed the linear relation of children's performance in the Delay of Gratification task with cortical surface area and thickness on the whole cortical surface. No significant correlation was found with either surface area or cortical thickness on the whole-brain level. In a next step, we then tested whether children's "hot" IC performance was related to cortical structure in our *a priori* defined ROIs. Using small-volume correction within the regions of the sCCN, PFC, and OFC, we found a significant positive relation of children's "hot" IC performance with their cortical surface area in the left supramarginal gyrus ($r = 0.22$, clusterwise $p = 0.017$; Table 1; Fig. 1*B*), and no significant relations in the PFC or OFC. Again, the effect remained significant when controlling for chronological age and gender.

Dissociation of "cold" and "hot" IC

To test for the independence of the effects observed for "cold" and "hot" IC, we additionally controlled for performance in the

Table 1. MNI coordinates, effect size, exact significance, and cluster size of significant relations between IC performance and cortical surface area[a]

	Anatomical region	Peak voxel coordinate in MNI 305 space (*x*, *y*, *z*)			Correlation (peak voxel)	Cluster wise *p* value	Cluster size (mm^2)
Whole-brain analysis							
"Cold" IC							
	L RFC	−35.4	57.1	−6.2	0.431	0.00459	687.43
	L inferior temporal lobe	−63.3	−43.2	−20.2	0.544	0.00978	628.70
	L precentral gyrus[b]	−28.6	−22.0	59.0	0.454	0.02247	550.10
	R PCC[b]	13.6	−23.9	35.9	0.480	0.00938	614.13
Small-volume correction: sCCN							
"Cold" IC							
	L RFC[b]	−33.1	56.2	−2.1	0.341	0.00020	376.86
	R RFC[b]	32.2	53.8	−4.7	0.358	0.00060	209.65
	R IPL[b]	44.0	−61.2	45.2	0.390	0.01460	136.17
"Hot" IC							
	L SMG[b]	−51.5	−49.8	59.0	0.216	0.01720	113.21
Small-volume correction: PFC							
"Cold" IC							
	L RFC[b]	−35.4	57.1	−6.2	0.420	0.00010	687.43
	R RFC[b]	38.0	58.8	−7.1	0.387	0.03790	217.05
	R caudal ACC	8.7	40.0	9.7	0.459	0.00120	374.78

[a]All effects are controlled for children's chronological age and gender. PCC, Posterior cingulate cortex; SMG, supramarginal gyrus.
[b]Regions were independent from the other IC domain.

other task, respectively. This showed that the regions of significant relation with "cold" IC performance in bilateral RFC and right IPL were independent of "hot" IC performance. Similarly, the "hot" IC effect observed in the supramarginal gyrus was independent of "cold" IC performance. Only the effect in caudal ACC did not remain significant when controlling for "hot" IC performance.

Analysis of subcortical brain structure

To test whether IC performance was related to subcortical brain structure, we performed nonparametric partial correlational analysis, relating IC performance with the reconstructed volume of the thalamus and striatal areas, while controlling for age, gender, and estimated total intracranial volume. We observed a positive correlation between children's "cold" IC performance and the volume of the left thalamus (Spearman's $\rho = 0.42$, $p = 0.013$; Fig. 1*C*), whereas "hot" IC performance was significantly related to the volume of the right thalamus (Spearman's $\rho = 0.37$, $p = 0.013$; Fig. 1*C*). The effect of "cold" IC in the left thalamus remained significant after controlling for "hot" IC performance. No significant correlation was found with the volume of striatal regions for "hot" and "cold" IC.

Analysis of WM connectivity

To investigate the structural connectivity of cortical and subcortical regions that were associated with "hot" and "cold" IC, respectively, we performed probabilistic tractography seeding in those regions. This analysis yielded a bilateral frontoparietal structural network connected to the cortical seed regions whose cortical structure had shown a linear relation to "cold" and "hot" IC performance (see Fig. 2*A*,*B*). In particular, seeding from clusters in the RFC and IPL clusters, we observed WM structures, such as the superior longitudinal fasciculus (SLF) and inferior fronto-occipital fasciculus, connecting the PFC with temporoparietal regions. Through seeding in the caudal ACC, we observed structures, such as the cingulum and corpus callosum. Further, seeding in the thalamus, we identified thalamocortical structural connections in both hemispheres (Fig. 2*C*). Additionally, we obtained frontostriatal connections through seeding in the OFC and using inclusion ROIs in the striatum (Fig. 3).

Next, we wanted to specify how and where structural connectivity in these tracts was related to children's IC abilities. To this end, we correlated streamline densities obtained from tractography with the children's IC performance, while controlling for children's age, gender, and surface area/volume of the seed region (see Materials and Methods for details). This showed a significant correlation of "cold" IC performance with streamline density in the dorsolateral PFC indexing higher connectivity to this region from the seed in the IPL along the right SLF ($r = 0.47$, $p = 0.002$) (Fig. 4*B*; Table 2). Furthermore, there were significant correlations of "cold" inhibitory functioning with streamline densities along the major forceps (Cluster 1: $r = 0.47$, $p = 0.023$; Cluster 2: $r = 0.46$, $p < 0.001$) and in the left corticospinal tract ($r = 0.44$, $p = 0.007$), which connects the left thalamus with the motor cortex (Fig. 4*A*; Table 2), independently of "hot" IC performance. For "hot" IC, we obtained a significant correlation with streamline density of the right superior and posterior thalamic radiation indexing higher connectivity from the seed in the right thalamus to the frontoparietal and occipital cortex ($r = 0.42$, $p = 0.001$; Fig. 4*C*; Table 2). No significant correlation was obtained for "hot" IC performance with streamline density of frontostriatal connections.

Discussion

IC constitutes a key prerequisite for humans to engage in goal-directed and adaptive behavior. A milestone of this ability is reached in the preschool period, between the ages of 3 and 4 years. What are the brain structures related to this core faculty in human cognitive development? To address this question, we studied structural brain markers of GM and WM maturation in relation to different facets of early IC cross-sectionally at the critical age of 3-4 years. We found that the behavioral breakthrough in IC was associated with structural indices of maturation in the cognitive control network, previously identified in adults (Niendam et al., 2012) and older children (McKenna et al., 2017). Distinct components of the cognitive control network were related to the different facets of IC: A standard

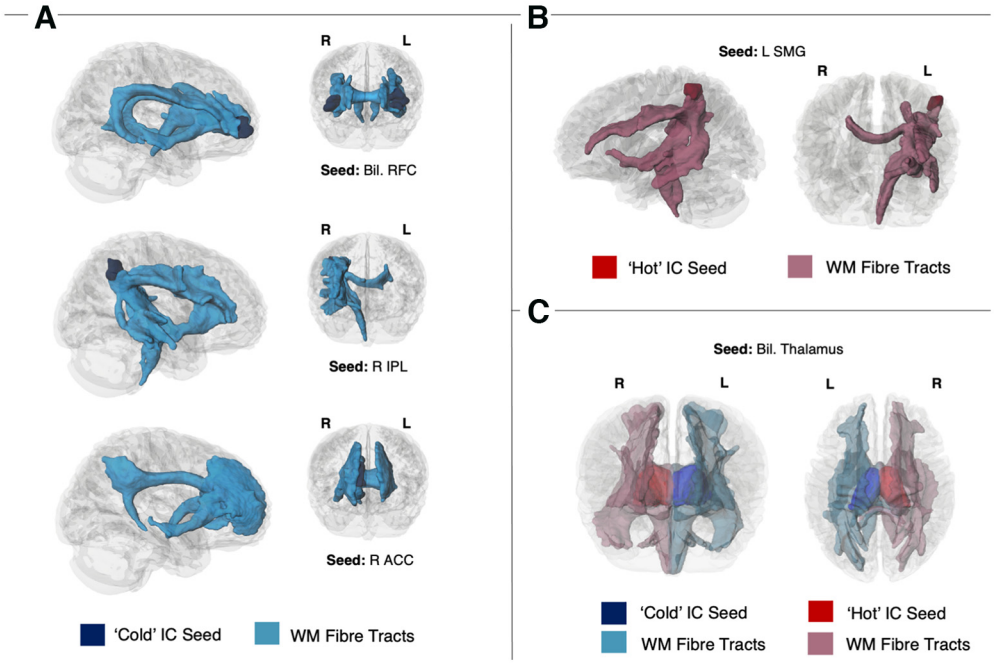

Figure 2. Streamline density maps resulting from probabilistic tractography seeded in brain regions showing a linear relation with "cold" (blue) and "hot" IC performance (red) on the cortical surface (***A*** and ***B***, respectively) and subcortical volume (bilateral thalamus, ***C***). SMG, Supramarginal gyrus.

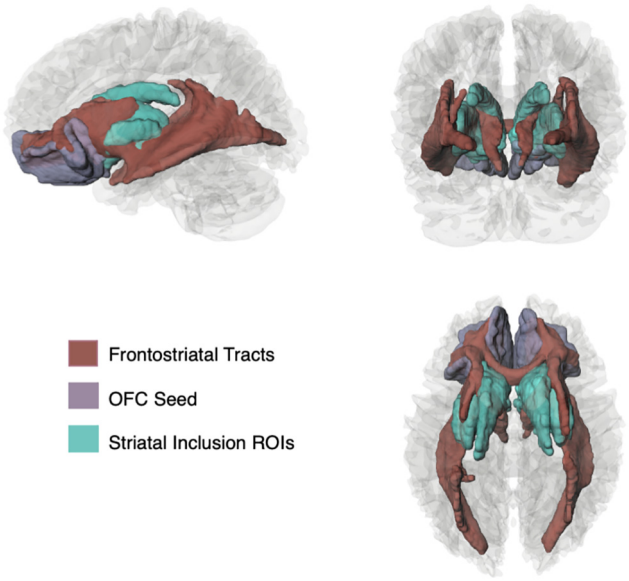

Figure 3. Streamline density map resulting from probabilistic tractography seeded in the OFC (gray), using inclusion ROIs in the striatum (green). The tractography revealed frontostriatal connections, along with the bilateral inferior fronto-occipital fasciculus (red).

cognitive ("cold") IC task was related to structure of the PFC, parietal lobe, and left thalamus, as well as frontoparietal and thalamocortical connections. A standard emotional ("hot") IC task, in contrast, was related to structural indices of maturation of the supramarginal gyrus, right thalamus, and distinct thalamocortical connections. These findings shed light on the brain structures associated with the emergence of IC, a central capacity for adaptive human behavior. Moreover, the independent brain networks involved in the different facets of IC support a dissociation of the structural networks underlying different task types thought to tap into "cold" and "hot" IC.

The emergence of "cold" IC in early childhood was associated with structural indices of maturation in core regions in the sCCN. More specifically, surface area in prefrontal (i.e., ACC, bilateral RFC) and parietal cortices (i.e., right inferior parietal lobe), as well as volume of the left thalamus was related to the marked developmental improvement observed on classic "cold" IC tasks between 3 and 4 years. A similar brain network has previously been found to be functionally involved in mature "cold" IC tasks in adults and late childhood (Niendam et al., 2012; McKenna et al., 2017). These findings support that the breakthrough observed in "cold" IC measures in preschool children (Petersen et al., 2016), such as in variants of the Go-NoGo task, reflects a development toward mature cognitive control. Structural connectivity of the above regions implicated in the "cold" IC task revealed how these regions are integrated in structural networks. This analysis yielded both frontoparietal and thalamocortical pathways, connecting important hubs of the sCCN. In particular, performance in the Go-NoGo task was related to connectivity of the SLF connecting the dorsolateral PFC with the inferior parietal lobe, the posterior corpus callosum (i.e., major forceps) connecting the two hemispheres, and connections between the left thalamus and motor cortex through the left corticospinal tract. These results suggest that, in addition to brain structure in IC processing regions, the extent to which these regions are connected to each other and to the thalamus via association, projection, and commissural fibres is relevant for the emergence of mature IC. Our findings highlight the importance of WM fiber connections that enable communication between core regions of cognitive control in prefrontal and parietal cortices and the thalamus. In particular, the SLF has been shown to provide the PFC with information on visual space and visuomotor function processed in the inferior parietal cortices, which may contribute to the regulation of spatial attention (Mesulam, 1981; Posner et al., 1984; Bisley and Goldberg, 2003). The importance of the SLF for cognitive control is further supported by research on pathologic conditions, showing that structural connectivity of the SLF is altered in disorders, such as obsessive-

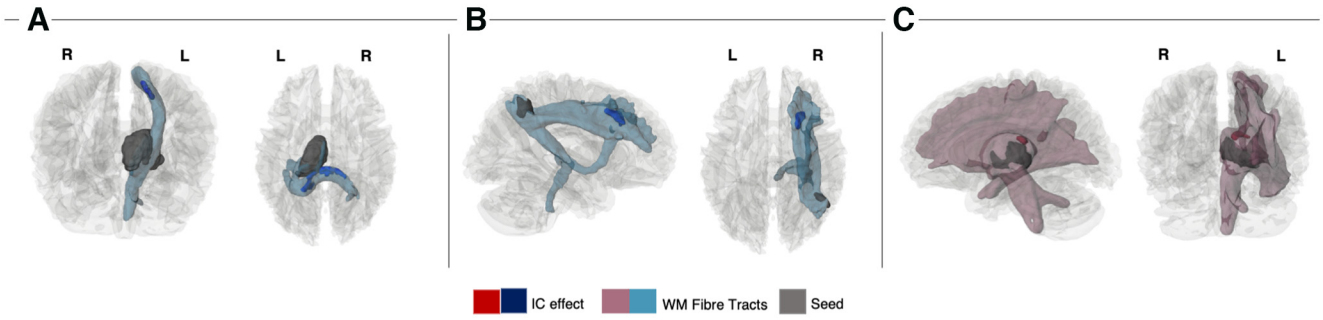

Figure 4. Correlation of streamline density with "cold" (blue) and "hot" IC performance (red). Results show a significant correlation of "cold" IC with streamline density in the left corticospinal tract and forceps major (***A***), and in the right SLF (***B***). "Hot" IC performance was correlated with streamline density of the right superior thalamic radiation (***C***). For visualization, WM visitation maps (light red, light blue) are restricted to streamlines that pass through the significant cluster. The effects were independent of children's age and gender, as well as surface area/volume of the seed region.

Table 2. MNI coordinates, effect size, exact significance, and cluster size of significant relations between IC performance and streamline density in WM tracts[a]

Seed region	Region of cluster	Tractography WM tracts	MNI coordinates center of gravity			Correlation coefficient	*p* value	Cluster size (voxels)
"Cold" IC								
R IPL	R DLPFC	R SLF	20.8	13.9	36.2	0.47	0.002[c]	127
L thalamus	CC	Major forceps[b]	4.9	−31.6	19.1	0.47	0.0230	123
L thalamus	CC	Major forceps	−13.3	−41.1	22.6	0.46	<0.001[c]	83
L thalamus	L PoCG	L corticospinal tract[b]	−14	−26.6	49.7	0.44	0.007[c]	60
"Hot" IC								
R thalamus	R thalamus	R thalamic radiation	10.9	−27.9	19.7	0.42	0.001[c]	64

[a]All effects are controlled for children's chronological age and gender, as well as surface area/volume of the respective seed region. DLPFC, Dorsolateral PFC; CC, corpus callosum; PoCG, postcentral gyrus.
[b]Regions independent from the other IC domain.
[c]*p* values surviving Bonferroni correction for the number of tracts.

compulsive disorder (Gan et al., 2017) and attention deficit/hyperactivity disorder (ADHD) (Hamilton et al., 2008; Gehricke et al., 2017). Specifically, research in ADHD has revealed that dysfunctional coupling in the SLF is associated with saccadic abnormalities (Fried et al., 2014; Matsuo et al., 2015) and increased response time variability (Wolfers et al., 2015). The corticospinal tract, in contrast, has functionally been linked to the control of voluntary movements (Kolb and Whishaw, 2009), and alterations of the corticospinal tract have been associated with the hyperactivity syndrome in ADHD (Bu et al., 2020). Our results therefore suggest that brain structures subserving different functional components of cognitive control, including attention regulation and motor control, are associated with young children's IC in neutral contexts.

In contrast to IC in neutral contexts, inhibition in an emotionally and motivationally high-stake situation, as assessed with the standard "hot" IC task, namely, the Delay of Gratification task (Mischel et al., 1989), was related to structural indices of maturation in brain regions of the sCCN that were distinct from those observed for the Go-NoGo task. These included the supramarginal gyrus and right thalamus. This distinction was confirmed by a double dissociation in that the main reported effects were independent of performance in the respective other IC domain. This was also supported by a distinct structural network for the Delay of Gratification task, which was associated with the connectivity of the right thalamus with frontoparietal and occipital cortices via the superior and posterior thalamic radiation. Through ascending and descending tracts from the cerebral cortex, the thalamic radiations integrate information throughout the brain, and are known to play a role in cognitive control and attention (Chaddock-Heyman et al., 2013; Stave et al., 2017; Brandes-Aitken et al., 2019).

In adults, the OFC and frontostriatal connections had previously been found to be functionally involved in IC in motivationally or emotionally laden situations that require the inhibition of direct incentive needs to achieve a higher-value reward (Casey et al., 2011; Achterberg et al., 2016). In preschoolers, however, maturational indices of these structures were not significantly associated with performance in the Delay of Gratification task. This was further confirmed by an additional analysis focusing only on frontostriatal structures, but yielding no significant correlation of streamline density obtained from the tractography with children's Delay of Gratification. Our data thus suggest that Delay of Gratification observed in the critical age range between 3 and 4 years is related to distinct components of the sCCN, rather than to a network specific for mature "hot" IC. Indeed, in addition to the representation of incentive value emphasized in adults, "hot" IC is thought to require the cognitive control of approach-avoidance tendencies (Zelazo and Carlson, 2020). For example, to master the Delay of Gratification task, children must not only represent and navigate between the values of immediate and delayed rewards, but also be able to suppress their motor responses appropriately and, if necessary, reorient their attention in a different direction to achieve the goal. Our finding that structural indices of the supramarginal gyrus, a region implicated in attentional control (Corbetta et al., 2008), and cortical connections of the thalamus to parietal regions and the motor cortex are related to early "hot" IC suggests that controlling approach-avoidance tendencies may be critical for the emergence of this ability in early childhood. Whether and from which age the maturation of frontostriatal connections (Casey et al., 2011; Achterberg et al., 2016) may be relevant to the early development of "hot" IC abilities remain a question for future investigation.

The observed differences in the structural networks related to "cold" and "hot" IC, respectively, are in line with evidence

showing low behavioral associations of IC in "hot" and cold' task situations but synchronous development of the two capacities (Willoughby et al., 2011; Zelazo and Carlson, 2012; Montroy et al., 2019). Moreover, this is consistent with a dissociation of these abilities observed in clinical populations (Bechara, 2004; Eslinger et al., 2004) and developmental disorders, such as ADHD, which has been found to differentially impair "hot" and "cold" IC performances (Hobson et al., 2011; Antonini et al., 2015). On the neural level, our brain-structural results complement recent findings from a functional near-infrared spectroscopy study by Moriguchi (2022), showing that PFC activation during "cold" IC tasks was generally stronger and uncorrelated to activation in the classical "hot" Delay of Gratification task. Together, these findings corroborate that the neural basis of "hot" and "cold" IC may differ in early childhood.

Notably, however, in light of the increasingly consistent findings supporting a dissociation of "hot" and "cold" IC abilities on the behavioral, neural, and clinical level, it is crucial to consider the inconsistencies in the way "hot" and "cold" IC are defined and studied. In particular, because of their different research backgrounds, standard "cold" and "hot" inhibition tasks, such as the Go-NoGo task and the Delay of Gratification task, do not only differ in the level of emotion or motivation included. They also show fundamental differences on many other factors in the task design (Simpson and Carroll, 2019). Different possibilities to conceptualize the differences between these tasks have been suggested in the developmental literature, such as, "conflict" versus "delay"-based inhibition (Carlson and Moses, 2001), or, "strength" versus "endurance"-based inhibition (Simpson and Carroll, 2019). Against this background, the question arises whether the observed dissociation of "hot" and "cold" IC may reflect other differences captured by these tasks. Future research could use several tasks for the IC domains to weaken the influence of task designs. However, to fully address this question in future research, it might be necessary to go beyond the traditional "hot-cold" distinction, which relies on differences in the operationalization of "hot" and "cold" executive functions (Zelazo and Carlson, 2012). Instead, the influence of emotion and motivation on inhibitory processing may be studied as a factor within the same task. This would ensure that task requirements do not differ besides the level of emotion included. Previous research in adults found that the ventral ACC modulated the influence of emotion on IC with such task designs (Kanske and Kotz, 2011; Kanske, 2012). Recently, similar tasks have been developed for preschool children (Berger and Grosse Wiesmann, 2021) and older children (Zinchenko et al., 2019). These tasks could be used to study associated brain maturation with a similar approach as the one used in the present study.

In conclusion, the present findings suggest that cortical and subcortical structure of core regions in the adult cognitive control network is related to early inhibitory functioning in preschool children. Further, our findings highlight the importance of frontoparietal (i.e., the superior longitudinal fascicle) and thalamocortical connections for early IC. Notably, however, the observed associations to brain structure were distinct for different facets of early IC, previously suggested in the behavioral literature (Zelazo and Carlson, 2012; Simpson and Carroll, 2019).

References

Achterberg M, Peper JS, van Duijvenvoorde AC, Mandl RC, Crone EA (2016) Frontostriatal white matter integrity predicts development of Delay of Gratification: a longitudinal study. J Neurosci 36:1954–1961.

Antonini TN, Becker SP, Tamm L, Epstein JN (2015) Hot and cool executive functions in children with attention deficit/hyperactivity disorder and comorbid oppositional defiant disorder. J Int Neuropsychol Soc 21:584–595.

Avants BB, Epstein CL, Grossman M, Gee JC (2008) Symmetric diffeomorphic image registration with cross-correlation: evaluating automated labeling of elderly and neurodegenerative brain. Med Image Anal 12:26–41.

Backhausen LL, Herting MM, Buse J, Roessner V, Smolka MN, Vetter NC (2016) Quality control of structural MRI images applied using FreeSurfer: a hands-on workflow to rate motion artifacts. Front Neurosci 10:558.

Bechara A (2004) The role of emotion in decision-making: evidence from neurological patients with orbitofrontal damage. Brain Cogn 55:30–40.

Benjamini Y, Hochberg Y (1995) Controlling the false discovery rate: a practical and powerful approach to multiple testing. J R Stat Soc B (Methodological) 57:289–300.

Berger P, Grosse Wiesmann C (2021) Positive emotion enhances conflict processing in preschoolers. Dev Sci e13199.

Bisley JW, Goldberg ME (2003) Neuronal activity in the lateral intraparietal area and spatial attention. Science 299:81–86.

Brandes-Aitken A, Anguera JA, Chang YS, Demopoulos C, Owen JP, Gazzaley A, Mukherjee P, Marco EJ (2019) White matter microstructure associations of cognitive and visuomotor control in children: a sensory processing perspective. Front Integr Neurosci 12:65.

Bu X, Yang C, Liang K, Lin Q, Lu L, Zhang L, Li H, Gao Y, Tang S, Hu X, Wang Y, Hu X, Wang M, Huang X (2020) Quantitative tractography reveals changes in the corticospinal tract in drug-naive children with attention-deficit/hyperactivity disorder. J Psychiatry Neurosci 45:134–141.

Buss AT, Spencer JP (2018) Changes in frontal and posterior cortical activity underlie the early emergence of executive function. Dev Sci 21:e12602.

Cafiero R, Brauer J, Anwander A, Friederici AD (2019) The concurrence of cortical surface area expansion and white matter myelination in human brain development. Cereb Cortex 29:827–837.

Carlson SM, Moses LJ (2001) Individual differences in inhibitory control and children's theory of mind. Child Dev 72:1032–1053.

Casey BJ, Somerville LH, Gotlib IH, Ayduk O, Franklin NT, Askren MK, Jonides J, Berman MG, Wilson NL, Teslovich T, Glover G, Zayas V, Mischel W, Shoda Y (2011) Behavioral and neural correlates of Delay of Gratification 40 years later. Proc Natl Acad Sci USA 108:14998–15003.

Chaddock-Heyman L, Erickson KI, Voss MW, Powers JP, Knecht AM, Pontifex MB, Drollette ES, Moore RD, Raine LB, Scudder MR, Hillman CH, Kramer AF (2013) White matter microstructure is associated with cognitive control in children. Biol Psychol 94:109–115.

Corbetta M, Patel G, Shulman GL (2008) The reorienting system of the human brain: from environment to theory of mind. Neuron 58:306–324.

Desikan RS, Ségonne F, Fischl B, Quinn BT, Dickerson BC, Blacker D, Buckner RL, Dale AM, Maguire RP, Hyman BT, Albert MS, Killiany RJ (2006) An automated labeling system for subdividing the human cerebral cortex on MRI scans into gyral based regions of interest. Neuroimage 31:968–980.

Eslinger PJ, Flaherty-Craig CV, Benton AL (2004) Developmental outcomes after early prefrontal cortex damage. Brain Cogn 55:84–103.

Feinberg DA, Moeller S, Smith SM, Auerbach E, Ramanna S, Gunther M, Glasser MF, Miller KL, Ugurbil K, Yacoub E (2010) Multiplexed echo planar imaging for sub-second whole brain fMRI and fast diffusion imaging. PLoS One 5:e15710.

Fischl B, Dale AM (2000) Measuring the thickness of the human cerebral cortex from magnetic resonance images. Proc Natl Acad Sci USA 97:11050–11055.

Fiske A, Holmboe K (2019) Neural substrates of early executive function development. Dev Rev 52:42–62.

Fried M, Tsitsiashvili E, Bonneh YS, Sterkin A, Wygnanski-Jaffe T, Epstein T, Polat U (2014) ADHD subjects fail to suppress eye blinks and microsaccades while anticipating visual stimuli but recover with medication. Vision Res 101:62–72.

Gan J, Zhong M, Fan J, Liu W, Niu C, Cai S, Zou L, Wang Y, Wang Y, Tan C, Chan RC, Zhu X (2017) Abnormal white matter structural connectivity in adults with obsessive-compulsive disorder. Transl Psychiatry 7:e1062.

Gehricke JG, Kruggel F, Thampipop T, Alejo SD, Tatos E, Fallon J, Muftuler LT (2017) The brain anatomy of attention-deficit/hyperactivity disorder in young adults: a magnetic resonance imaging study. PLoS One 12: e0175433.

Greve DN, Fischl B (2018) False positive rates in surface-based anatomical analysis. Neuroimage 171:6–14.

Grosse Wiesmann C, Friederici AD, Singer T, Steinbeis N (2017a) Implicit and explicit false belief development in preschool children. Dev Sci 20: e12445.

Grosse Wiesmann C, Schreiber J, Singer T, Steinbeis N, Friederici AD (2017b) White matter maturation is associated with the emergence of Theory of Mind in early childhood. Nat Commun 8:10.

Grosse Wiesmann C, Friederici AD, Singer T, Steinbeis N (2020) Two systems for thinking about others' thoughts in the developing brain. Proc Natl Acad Sci USA 117:6928–6935.

Halassa MM, Kastner S (2017) Thalamic functions in distributed cognitive control. Nat Neurosci 20:1669–1679.

Hamilton LS, Levitt JG, O'Neill J, Alger JR, Luders E, Phillips OR, Caplan R, Toga AW, McCracken J, Narr KL (2008) Reduced white matter integrity in attention-deficit hyperactivity disorder. Neuroreport 19:1705–1708.

Hobson CW, Scott S, Rubia K (2011) Investigation of cool and hot executive function in ODD/CD independently of ADHD. J Child Psychol Psychiatry 52:1035–1043.

Jenkinson M, Bannister P, Brady M, Smith S (2002) Improved optimization for the robust and accurate linear registration and motion correction of brain images. Neuroimage 17:825–841.

Johansen-Berg H (2010) Behavioural relevance of variation in white matter microstructure. Curr Opin Neurol 23:351–358.

Kanske P (2012) On the influence of emotion on conflict processing. Front Integr Neurosci 6:42.

Kanske P, Kotz SA (2011) Emotion triggers executive attention: anterior cingulate cortex and amygdala responses to emotional words in a conflict task. Hum Brain Mapp 32:198–208.

Kim S (2015) ppcor: partial and Semi-Partial (Part) correlation. Available at https://CRAN.R-project.org/package=ppcor.

Kolb B, Whishaw IQ (2009) Fundamentals of human neuropsychology. New York: Macmillan.

Marques JP, Kober T, Krueger G, van der Zwaag W, Van de Moortele PF, Gruetter R (2010) MP2RAGE, a self bias-field corrected sequence for improved segmentation and T1-mapping at high field. Neuroimage 49:1271–1281.

Matsuo Y, Watanabe M, Taniike M, Mohri I, Kobashi S, Tachibana M, Kobayashi Y, Kitamura Y (2015) Gap effect abnormalities during a visually guided pro-saccade task in children with attention deficit hyperactivity disorder. PLoS One 10:e0125573.

McKenna R, Rushe T, Woodcock KA (2017) Informing the structure of executive function in children: a meta-analysis of functional neuroimaging data. Front Hum Neurosci 11:154.

Mehnert J, Akhrif A, Telkemeyer S, Rossi S, Schmitz CH, Steinbrink J, Wartenburger I, Obrig H, Neufang S (2013) Developmental changes in brain activation and functional connectivity during response inhibition in the early childhood brain. Brain Dev 35:894–904.

Mesulam MM (1981) A cortical network for directed attention and unilateral neglect. Ann Neurol 10:309–325.

Mischel W, Ebbesen EB (1970) Attention in Delay of Gratification. J Pers Soc Psychol 16:329–337.

Mischel W, Shoda Y, Rodriguez ML (1989) Delay of gratification in children. Science 244:933–938.

Montroy JJ, Merz EC, Williams JM, Landry SH, Johnson UY, Zucker TA, Assel M, Taylor HB, Lonigan CJ, Phillips BM, Clancy-Menchetti J, Barnes MA, Eisenberg N, Spinrad T, Valiente C, de Villiers J, de Villiers P (2019) Hot and cool dimensionality of executive function: model invariance across age and maternal education in preschool children. Early Child Res Q 49:188–201.

Moriguchi Y (2022) Relationship between cool and hot executive function in young children: a near-infrared spectroscopy study. Dev Sci 25:e13165.

Moriguchi Y, Shinohara I, Yanaoka K (2018) Neural correlates of Delay of Gratification choice in young children: near-infrared spectroscopy studies. Dev Psychobiol 60:989–998.

Niendam TA, Laird AR, Ray KL, Dean YM, Glahn DC, Carter CS (2012) Meta-analytic evidence for a superordinate cognitive control network subserving diverse executive functions. Cogn Affect Behav Neurosci 12:241–268.

Oishi K, Faria A, van Zijl PC, Mori S (2011) MRI atlas of human white matter. San Diego: Academic.

Petersen IT, Hoyniak CP, McQuillan ME, Bates JE, Staples AD (2016) Measuring the development of inhibitory control: the challenge of heterotypic continuity. Dev Rev 40:25–71.

Posner MI, Walker JA, Friedrich FJ, Rafal RD (1984) Effects of parietal injury on covert orienting of attention. J Neurosci 4:1863–1874.

R Core Team (2019) R: a language and environment for statistical computing. Vienna: R Foundation for Statistical Computing. Available at https://www.R-project.org/.

Rakoczy H (2010) Executive function and the development of belief-desire psychology. Dev Sci 13:648–661.

Raznahan A, Lerch JP, Lee N, Greenstein D, Wallace GL, Stockman M, Clasen L, Shaw PW, Giedd JN (2011) Patterns of coordinated anatomical change in human cortical development: a longitudinal neuroimaging study of maturational coupling. Neuron 72:873–884.

Rothbart MK, Posner MI (1985) Temperament and the development of self-regulation. In: The neuropsychology of individual differences, pp 93–123. Boston, MA: Springer.

Schreiber J, Riffert T, Anwander A, Knösche TR (2014) Plausibility tracking: a method to evaluate anatomical connectivity and microstructural properties along fiber pathways. Neuroimage 90:163–178.

Simpson A, Carroll DJ (2019) Understanding early inhibitory development: distinguishing two ways that children use inhibitory control. Child Dev 90:1459–1473.

Soares J, Marques P, Alves V, Sousa N (2013) A hitchhiker's guide to diffusion tensor imaging. Front Neurosci 7:31.

Somerville LH, Casey BJ (2010) Developmental neurobiology of cognitive control and motivational systems. Curr Opin Neurobiol 20:236–241.

Stave EA, De Bellis MD, Hooper SR, Woolley DP, Chang SK, Chen SD (2017) Dimensions of attention associated with the microstructure of corona radiata white matter. J Child Neurol 32:458–466.

Tournier JD, Calamante F, Gadian DG, Connelly A (2004) Direct estimation of the fiber orientation density function from diffusion-weighted MRI data using spherical deconvolution. Neuroimage 23:1176–1185.

Tournier JD, Mori S, Leemans A (2011) Diffusion tensor imaging and beyond. Magn Reson Med 65:1532–1556.

Tournier JD, Calamante F, Connelly A (2012) MRtrix: diffusion tractography in crossing fiber regions. Int J Imaging Syst Technol 22:53–66.

Walhovd KB, Fjell AM, Giedd J, Dale AM, Brown TT (2017) Through thick and thin: a need to reconcile contradictory results on trajectories in human cortical development. Cereb Cortex 27:1472–1481.

Willoughby MT, Wirth RJ, Blair CB (2011) Contributions of modern measurement theory to measuring executive function in early childhood: an empirical demonstration. J Exp Child Psychol 108:414–435.

Winkler AM, Ridgway GR, Webster MA, Smith SM, Nichols TE (2014) Permutation inference for the general linear model. Neuroimage 92:381–397.

Wolfers T, Onnink AM, Zwiers MP, Arias-Vasquez A, Hoogman M, Mostert JC, Kan CC, Slaats-Willemse D, Buitelaar JK, Franke B (2015) Lower white matter microstructure in the superior longitudinal fasciculus is associated with increased response time variability in adults with attention-deficit/hyperactivity disorder. J Psychiatry Neurosci 40:344–351.

Zelazo PD, Carlson SM (2012) Hot and cool executive function in childhood and adolescence: development and plasticity. Child Dev Perspect 6:360.

Zelazo PD, Carlson SM (2020) The neurodevelopment of executive function skills: implications for academic achievement gaps. Psychol Neurosci 13:273–298.

Zinchenko A, Chen S, Zhou R (2019) Affective modulation of executive control in early childhood: evidence from ERPs and a Go/Nogo task. Biol Psychol 144:54–63.